Available online at www.sciencedirect.com

ScienceDirect

Ceramics International 40 (2014) 1759–1763

CERAMICS INTERNATIONAL

www.elsevier.com/locate/ceramint

Pressureless sintered silicon carbide with enhanced mechanical properties obtained by the two-step sintering method

Giuseppe Magnani*, Alida Brentari, Emiliano Burresi, Giancarlo Raiteri

ENEA, UTTMATF, Faenza Research Laboratories, Bologna Research Center, Via Ravegnana, 186-48018 Faenza (RA), Italy

Received 2 May 2013; received in revised form 8 July 2013; accepted 15 July 2013
Available online 22 July 2013

Abstract

The Two-step sintering (TSS) method was applied to the pressureless sintering of commercial silicon carbide powder doped with boron and carbon. The microstructural and mechanical properties of TSS-SiC were compared to those of sintered SiC obtained with the conventional thermal cycle (CS-SiC). TSS-SiC was densified (97.7% T.D.) at 2050 °C instead of 2200 °C needed for CS-SiC (97% T.D.). Furthermore, TSS-SiC showed finer microstructure and enhanced mechanical properties. In particular, flexural strength of the TSS-SiC materials greatly increased up to 556 MPa, much higher than 341 MPa reached by CS-SiC.

Keywords: A. Sintering; C. Mechanical properties; D. SiC

1. Introduction

Silicon carbide (SiC) is a very interesting ceramic material due to its properties like high hardness, low bulk density, high oxidation resistance which make SiC suitable for a wide range of industrial applications. Sintering of silicon carbide was first performed by Prochazka [1] by using boron and carbon through a solid state mechanism (BC-SSiC). This process is normally performed at 2150–2200 °C and densification is enhanced through the reduction of the superficial energy of the grains promoted by boron [2] and the reaction between carbon and the silica film [2–4] located on the SiC particle surface.

The additives most widely used are boron and carbon and they normally cause an exaggerated grain growth due to the high sintering temperature needed to reach high sintered density. Pressureless sintering of BC-SSiC at lower temperature would be desirable in order to limit the grain growth, but it is still an unresolved issue. Coarse microstructure affects the mechanical properties and several sintering methods have been already tested with BC-SSiC in order to reduce the grain size and to improve the mechanical properties by using simultaneous pressure application during sintering (hot pressing, hot isostatic pressing and spark plasma sintering) [5–9] also with different additives (Al-B-C) [10] or through liquid phase mechanism (metal and rare-earth oxides) [11]. The main problems of the pressure-assisted sintering processes are high production costs and limitation in the product size and shape complexity which can limit the industrial applicability. Two-step pressureless sintering process can be proposed both to overcome these limitations and to reduce the sintering temperature in order to obtain high strength BC-SSiC ceramics with fine microstructure.

The two-step sintering method (TSS) proposed by Chen and Wang [12] is based on the heating of the sample to a high temperature T_1 followed by a rapid cooling down to a lower temperature T_2 and then held at T_2 for a long period. The main characteristic of this method is that the grain boundary diffusion of the sample is maintained avoiding at the same time the grain boundary migration. Therefore, the grain growth associated to the final step of the sintering process is completely suppressed. Several studies focused on this method are available. Chen and Wang [12] firstly applied this method in Y_2O_3 ceramics, whereas different authors were able to obtain $BaTiO_3$ [13], ZnO [14, 15], ZrO_2 [16–19], Al_2O_3–ZrO_2

*Corresponding author. Tel.: +39 0546 678583.
E-mail address: giuseppe.magnani@enea.it (G. Magnani).

0272-8842/$ - see front matter © 2013 Elsevier Ltd and Techna Group S.r.l. All rights reserved.
http://dx.doi.org/10.1016/j.ceramint.2013.07.075

[20], Al_2O_3 [21, 22] and SiC [23] ceramics. In particular, Lee et al. [23] obtained nanostructured SiC ceramics with a two-step liquid phase sintering process based on hot pressing with alumina, yttria and calcia as sintering aids. To our knowledge this is the only study focused on the TSS method applied to SiC, whereas there are no studies on the applicability of the TSS method on the pressureless sintering of the SiC-B-C system. On the basis of these considerations, the study reported in this paper was aimed to show that the two-step sintering method can be used to manufacture pressureless-sintered BC-SSiC ceramics at temperature lower than 2150–2200 °C. In addition, further scope was the evaluation of the effects of the TSS method on the mechanical properties.

2. Experimental procedure

Commercially available α-SiC (UF15 Premix, H.C. Starck, Germany) was used as starting powder. This is a ready-to-press powder with the appropriate amount of organic binder and sintering aids (boron and carbon). The main physical and chemical characteristics of the powder are reported in Table 1. Discs with diameter 35 mm and thickness 3 mm were prepared by uniaxial pressing at 60 MPa followed by cold isostatic pressing at 200 MPa. Sintering was performed in a graphite resistance high temperature furnace in flowing argon at 1 atm. The temperature of the conventional sintering (CS) was set at 2200 °C for 1 h, whereas TSS was conducted at 2100 °C (T_1) and 2050 °C (T_2) for a period of time up to 7 h.

Samples density (CS-SiC and TSS-SiC) were determined by the Archimedes method (ASTM C373). The microstructures of the polished and chemically etched (Murakami′s etching) samples were observed using scanning electron microscopy (SEM-LEO 438 VP). X-ray patterns (XRD) were collected with a Philips powder diffractometer with a Bragg–Brentano geometry and equipped with a copper anode operated at 40 kV and 30 mA (step 0.02°, time 6 s). The phase analysis was carried out with the PC X′pert High Score software Version 2.2a (PANalytical B.V., Almelo, The Netherlands).

The flexural strength was determined by four-point bending tests. Ten samples as bars of $2 \times 2.5 \times 25$ mm^3 were prepared and tested in accordance with the standard ENV 843-1 (crosshead speed 0.5 mm/min, support span 20 mm).

Table 1
Chemical and physical properties of the commercial powder.

Properties	UF15 premix
Specific surface area (m^2/g)	14–16
Bulk density (g/cm^3)	0.72
Granule size (μm)	< 150
Particle size distribution d_{90} (μm)	1.3
d_{50} (μm)	0.6
d_{10} (μm)	0.25
Oxygen (wt%)	< 1.5
Boron (wt%)	0.5
Carbon (wt%)	3.0
Organic binder (wt%)	< 10

The fracture toughness was calculated by the Vickers indentation method on the basis of the equation proposed by Niihara et al. [24]:

$$K_{IC} = 0.203\, Ha^{1/2}(c/a)^{-3/2} \quad (1)$$

where H is the hardness, a is the impression radius and c is the crack length. The indentations were performed with a load of 98 N.

Finally, the elastic modulus was determined by applying the impulse excitation method in accordance with the standard EN 843-2. Each sample, supported at its nodes for the fundamental frequency of flexural vibration, was lightly struck by a small hammer in order to detect its natural frequency of vibration by a microphone (or a piezo transducer) coupled to a proper frequency analyser. In the experimental activity here described, a microphone was used, connected to the frequency analyser Grindo-Sonic System Mk5-Industrial (J.W. Lemmens N.V., Belgium).

The values of Young′s modulus were then calculated in accordance with the following equation:

$$E = 0.946\,(mf^2/b)(l/h)^3[1 + 6.585(h/l)^2] \quad (2)$$

where E is the dynamic Young′s modulus, m the mass of the test piece, b the width of the test piece perpendicular to the flexural mode vibration, h the thickness of the test piece in direction of flexural vibration, l the length of the test piece and f the fundamental frequency of flexural vibration.

3. Results and discussion

3.1. Density and microstructure

Microstructures of the samples obtained with both methods, CS and TSS, are reported in Fig. 1. CS-SiC sample shows an exaggerated grain growth with grains having length more than 100 μm and very high aspect ratio. On the contrary, the microstructure of TSS-SiC sample is mainly composed of equiaxed grains with some elongated grains with length of about 30 μm. The residual porosity is homogeneously distributed in the CS-SiC and TSS-SiC samples having very similar sintered density: 97% T.D. and 97.7% T.D., respectively (T.D. = 3.2 g/cm^3). Conventional sintering was also tested at temperature lower than 2200 °C in order to limit the grain growth, but the density was always less than the value obtained at 2200 °C. These results confirmed that the second step of the TSS method performed at lower temperature than CS (2050 °C instead of 2200 °C) leads to the same final densification with limited grain growth. Furthermore, there are no reports that SiC ceramics can be densified at 2050 °C using the pressureless sintering process, boron–carbon additives and starting powder of similar quality.

The lowering of the sintering temperature from 2200 °C (CS) to 2050 °C (TSS) also influences the content of the different α-SiC polytypes. The XRD patterns reported in Fig. 2 show some peaks with different intensities. The quantitative determination of the content of the 6H, 4H and 15R polytypes was carried out on the basis of the method proposed by Ruska et al. [25] (Table 2). TSS-SiC sample showed a lower content

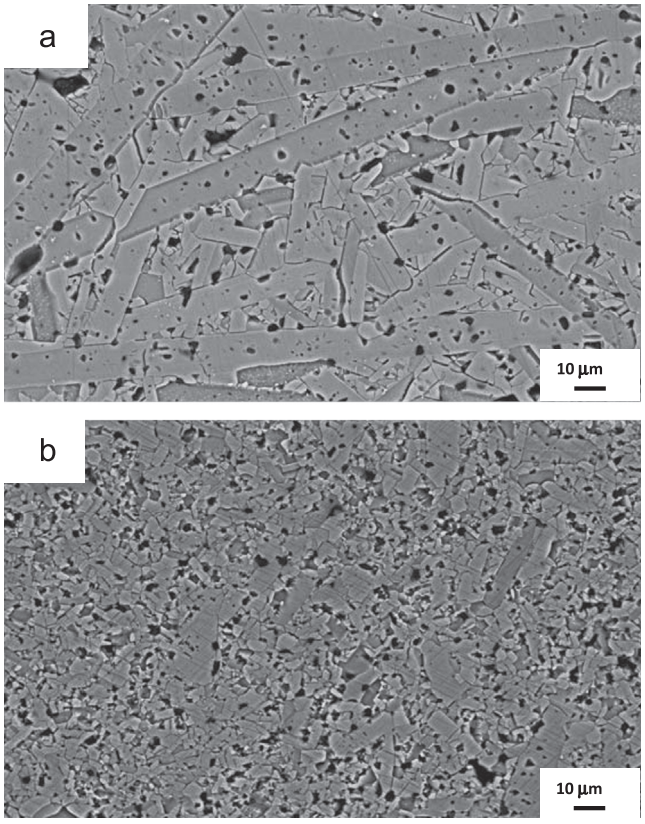

Fig. 1. Microstructure of the (a) CS-SiC and (b) TSS-SiC materials after chemical etching.

of 15R and an higher content of 6H than CS-SiC sample fired up to 2200 °C. The formation mechanisms and thermodynamic stability of all different polytypes are not clearly understood. It is believed that temperature, impurities, gas atmosphere and growth kinetic processes have an influence on the stability of the different polytypes. In any case, the results reported in Table 2 confirmed that 6H-SiC is stable below 2100 °C and 15 R above 2100 °C [26].

3.2. Mechanical properties

The mechanical properties (hardness, Young′s modulus, fracture toughness, flexural strength) of the CS-SiC and TSS-SiC materials are summarized in Table 3.

TSS-SiC and CS-SiC exhibited undistinguishable hardness and fracture toughness values. The hardness changes from 23.3 GPa (CS-SiC) to 24.4 GPa (TSS-SiC). These values were used to calculate the fracture toughness by using Eq. (1). Taking into account the limitations of the Vickers indentation method, the results reported in Table 3 can be considered as values of the "fracture resistance" of the two materials instead of fracture toughness. The difference between TSS-SiC and CS-SiC is not detectable and it is not possible to evaluate the effects of the grain size on the fracture resistance. Indentation tests were also performed in the load range 4.9–122.6 N in order to evaluate the variation of crack length as a function of indentation load. Fracture toughness can be determined using crack length (c) and indentation load (P) on the basis of the general equation proposed by Lawn et al. [27]:

$$K_{IC} = \chi P / c^{2/3} \quad (3)$$

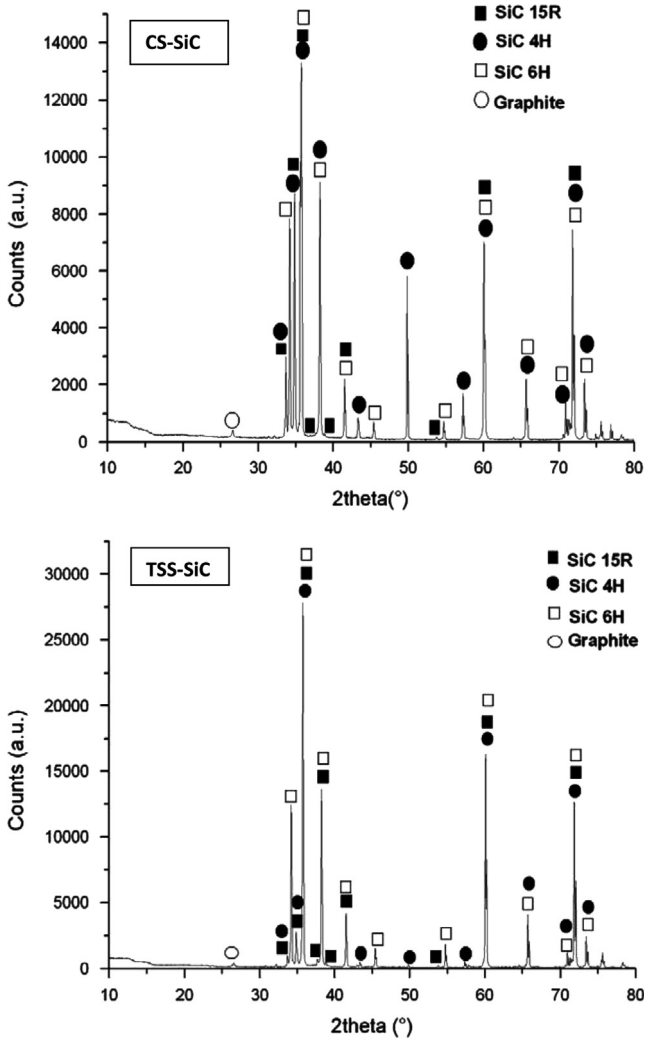

Fig. 2. XRD spectra of of CS-SiC and TSS-SiC materials.

Table 2
SiC polytypes content in CS-SiC and TSS-SiC ceramics.

Material	6H (%)	4H (%)	15R (%)
CS-SiC	26.4	23.0	50.6
TSS-SiC	84.7	10.0	5.3

Table 3
Mechanical properties (mean value ± deviation standard) of the investigated materials, CS-SiC and TSS-SiC. Indentation load = 98 N.

Mechanical properties	CS-SiC	TSS-SiC
Hardness (GPa)	23.3 ± 0.7	24.4 ± 0.7
Fracture toughness (MPa $m^{1/2}$)	3.1 ± 0.2	3.4 ± 0.1
Young modulus (GPa)	409 ± 1	418 ± 2
Flexural strength (MPa)	341 ± 43	556 ± 56

where χ is a constant. By applying the logarithm to both sides of Eq. (3), linear relationship between log c and log P can be obtained.

In the case of CS-SiC and TSS-SiC Eq. (3) can be re-written as reported in Eqs. 4 and 5, respectively:

$$\log c = 0.633\text{Log } P + 1.022 \quad (4)$$

$$\log c = 0.658\log P + 0.972 \quad (5)$$

where slope and intercept were obtained by applying the least-square method (Fig. 3). Furthermore, the slopes resulted very close to the theoretical value of 0.67 indicating that radial cracks observed on the surface correspond to the median crack [24,28].

SEM observations of the fracture surfaces (Fig. 4) put in evidence different fracture modes: TSS-SiC shows a mixed intergranular–transgranular fracture mode (Fig. 4a), whereas CS-SiC presents typical transgranular fracture mode (Fig. 4b). Furthermore, examination of the crack propagation clearly showed transgranular fracture without any deflection in CS-SiC, whereas TSS-SiC exhibits crack deflection and grain bridging (Fig. 5).

The investigated materials showed different elastic moduli. It is well known that it is strictly influenced by the porosity, whereas neither grain size nor polytype was recognized as having a significant effect on the elastic modulus of SiC. The variation of the elastic modulus as a function of porosity can be evaluated by the equation proposed by Snead et al. [29]:

$$E = E_0\exp(-CV_P) \quad (6)$$

where V_P is the residual porosity, E_0 is the elastic modulus of the pore free SiC (460 GPa) [29] and C is a constant (3.57). E values calculated on the basis of the Eq. (6), 424 GPa and 414 GPa for TSS-SiC and CS-SiC respectively, are in accordance with those obtained experimentally considering that the uncertainty of the elastic modulus of SiC is $\pm 15\%$ with $V_P > 1\%$ [29].

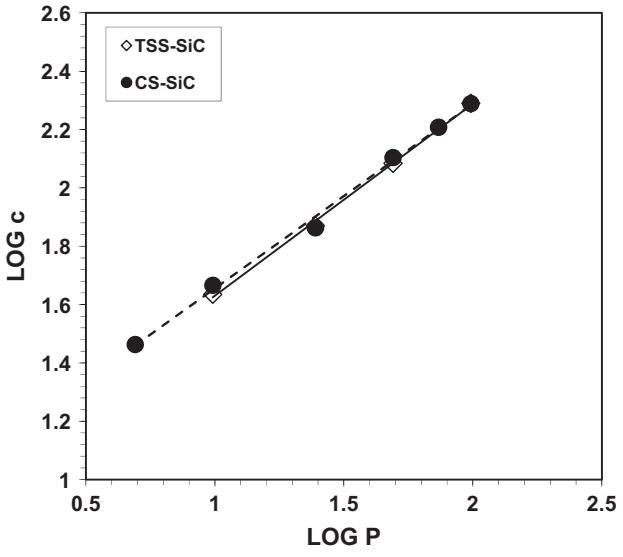

Fig. 3. Log–log relationship between crack length c (μm) as a function of the indentation load P (N).

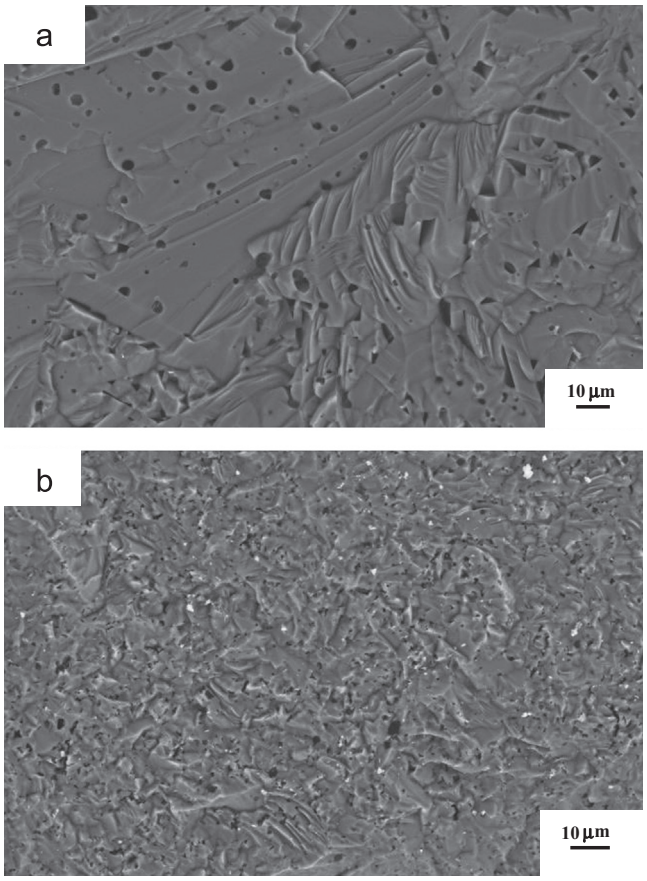

Fig. 4. Fracture surface of (a) CS-SiC and (b) TSS-SiC materials showing different fracture modes.

Flexural strength at room temperature of the two materials is significantly different with TSS-SiC ceramics having higher mean flexural strength (556 MPa) than CS-SiC (341 MPa). This difference was also evident at 1500 °C with mean values of 542 MPa and 267 MPa for TSS-SiC and CS-SiC, respectively. Four-point bending fracture strength of brittle ceramic is highly dependent on the size of the largest flaw in the part of the sample under tension. The higher strength of the TSS-SiC material are related to the decreasing importance of critical flaw size on strength. The critical flaw size could be calculated by the modified Griffith's equation [30]:

$$K_{IC} = 1.23\sigma_f c^{1/2} \quad (7)$$

where K_{IC}, σ_f and c are the fracture toughness, strength and critical flaw size, respectively. The results confirmed that TSS-SiC sample has smaller critical flaw size (25 μm) than CS-SiC sample (55 μm).

4. Conclusion

Commercial SiC powder doped with boron and carbon was densified with the two-step sintering method. TSS-SiC was obtained at 2050 °C and showed finer microstructure than conventional sintered SiC fired at 2200 °C. The reducing of the grain size greatly influenced flexural strength, whereas hardness and fracture resistance remained substantially constant.

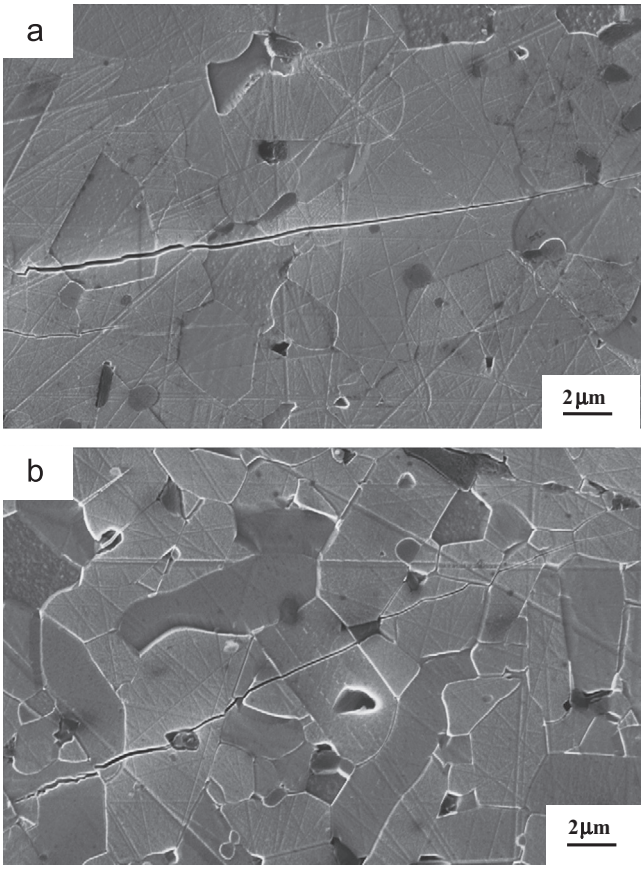

Fig. 5. SEM micrographs of the crack propagation in (a) CS-SiC and (b) TSS-SiC.

In addition, TSS-SiC showed mixed transgranular–intergranular fracture mode, whereas CS-SiC presented transgranular fracture mode. TSS-SiC also exhibited a slight higher density than CS-SiC and it is responsible for the differences in the elastic modulus.

References

[1] S. Prochazka, Hot Pressed Silicon Carbide, US Patent 3853566, 10 December 1974.
[2] E.R. Maddrell, Pressureless sintering of silicon carbide, Journal of Materials Science Letters 6 (1987) 486–488.
[3] W. Van Rijswjk, D.J. Shanafeld, Effects of carbon as a sintering aid in silicon carbide, Journal of the American Ceramic Society 73 (1990) 148–149.
[4] R. Hamminger, Carbon inclusions in sintered silicon carbide, Journal of the American Ceramic Society 72 (1989) 1741–1744.
[5] L. Vargas-Gonzalez, R.F. Speyer, J. Campbell, Flexural strength, fracture toughness, and hardness of silicon carbide and boron carbide armor ceramics, International Journal of Applied Ceramic Technology 7 (2010) 643–651.
[6] S. Hayun, V. Paris, R. Mitrani, S. Kalabukhov, M.P. Dariel, E. Zaretsky, N. Frage, Microstructure and mechanical properties of silicon carbide processed by Spark Plasma Sintering (SPS), Ceramics International 38 (2012) 6335–6340.
[7] T.A. Yamamoto, T. Kondou, Y. Kodera, T. Ishii, M. Ohyanagi, Z.A. Munir, Mechanical properties of β-SiC fabricated by spark plasma sintering, Journal of Materials Engineerign and Performance 14 (2005) 460–466.
[8] C. Lorrette, A. Réau, L. Briottet, Mechanical properties of nanostructured silicon carbide consolidated by spark plasma sintering, Journal of the European Ceramic Society 33 (2013) 147–156.
[9] S. Dutta, Improved processing of α-SiC, Advanced Ceramic Materials 3 (1988) 257–262.
[10] J.J. Cao, W.J. Moberly Chan, L.C. De Jonghe, C.J. Gilbert, R.O. Ritchie, In situ toughened silicon carbide with Al-B-C additions, Journal of the American Ceramic Society 79 (1996) 461–469.
[11] M. Omori, H. Takei, Preparation of pressureless-sintered SiC–Y_2O_3–Al_2O_3, Journal of Materials Science 23 (1988) 3744–3749.
[12] I.W. Chen, X.H. Wang, Sintering dense nanocrystalline ceramics without final-stage grain growth, Nature 404 (2000) 168–171.
[13] A. Polotai, K. Breece, E. Dickey, C. Randall, A. Ragulya, A novel approach to sintering nanocrystalline barium titanate ceramics, Journal of the American Ceramic Society 88 (2005) 3008–3012.
[14] P. Duran, F. Capel, J. Tartaj, C. Moure, A strategic two-stage low temperature thermal processing leading to fully dense and fine-grained doped-ZnO varistors, Advanced Materials 14 (2002) 137–141.
[15] S.P. Lee, B. Hwang, Y.K. Paek, T.J. Chung, S.H. Yang, S. Lim, W.S. Seo, K.S. Oh, Determination of the initial heat treatment temperature in the two-step sintering of xAl–ZnO (x=1, 2, and 3 wt%), Journal of the European Ceramic Society 33 (2013) 131–137.
[16] M. Mazaheri, A. Simchi, F. Golestani-Fard, Densification and grain growth of nanocrystalline 3Y-TZP during two-step sintering, Journal of the European Ceramic Society 28 (2008) 2933–2939.
[17] G. Suárez, Y. Sakka, T.S. Suzuki, T. Uchikoshi, X. Zhu, E.F. Aglietti, Effect of starting powders on the sintering of nanostructured ZrO_2 ceramics by colloidal processing, Science and Technology of Advanced Materials 10 (2009) 025004 (8pp.).
[18] E.N.S. Muccillo, R. Muccillo, Effect of processing methodology on microstructure and ionic conductivity of yttria-stabilized zirconia, ECS Transactions 28 (2010) 325–331.
[19] M.A. Lourenco, G.G. Cunto, F.M. Figueiredo, J.R. Frade, Model of two-step sintering conditions for yttria.substituted zirconia powder, Materials Chemistry and Physics 126 (2011) 262–271.
[20] C.J. Wang, C.Y. Huang, Y.C. Wu, Two-step sintering of fine alumina-zirconia ceramics, Ceramics International 35 (2009) 1467–1472.
[21] K. Bodigova´, P. Sajgalìk, D. Galusek, P. Svancarek, Two-stage sintering of alumina with submicrometer grain size, Journal of the American Ceramic Society 90 (2007) 330–332.
[22] D. Galusek, K. Ghillanyova, J. Sedlacek, J. Kozankova, P. Sajgalìk, The influence of additives on microstructure of sub-micron alumina ceramics prepared by two-stage sintering, Journal of the European Ceramic Society 32 (2012) 1965–1970.
[23] Y.I. Lee, Y.M. Kim, M. Mitomo, D.Y. Kim, Fabrication of dense nanostructured silicon carbide ceramics through two-step sintering, Journal of the American Ceramic Society 86 (2003) 1803–1805.
[24] K. Niihara, A. Nakahira, T. Hirai, The effect of stoichiometry on mechanical properties of boron carbide, Journal of the American Ceramic Society 67 (1984) C13–C14.
[25] J. Ruska, L.J. Gauckler, J. Lorenz, H.U. Rexer, The quantitative calculation of SiC polytypes from measurements of X-ray diffraction peak intensities, Journal of Materials Science 14 (1979) 2013–2017.
[26] Y. Inomata, Z. Inoue, M. Mitomo, Thermal stability of 6H and 15R types of SiC, Journal of Crystal Growth 5 (1969) 405–407.
[27] B.R. Lawn, A.G. Evans, D.B. Marshall, Elastic/plastic indentation damage in ceramics: the median/radial crack system, Journal of the American Ceramic Society 63 (1980) 574–581.
[28] K.M. Liang, G. Orange, G. Fantozzi, Evaluation by indentation of fracture toughness of ceramic materials, Journal of Materials Science 25 (1990) 207–214.
[29] L.L. Snead, T. Nozawa, Y. Katoh, T.S. Byun, S. Kondo, D.A. Petti, Handbook of SiC properties for fuel performance modeling, Journal of Nuclear Materials 371 (2007) 329–377.
[30] O.R. Chakrabarti, S. Ghosh, J. Mukerji, Influence of grain size, free silicon content and temperature on the strength and toughness of reaction-bonded silicon carbide, Ceramics International 20 (1994) 283–286.